Journal of Non Crystalline Solids. Vol. 353. Núm. 8-10. 2007. Pag. 872-874
http://dx.doi.org/10.1016/j.jnoncrysol.2006.12.097

Thermal and microstructural stability of the soft magnetic $Fe_{60}Co_{18}Nb_6B_{15}Cu_1$ alloy

J. S. Blázquez,[a] V. Franco[a], C. F. Conde[a], A. Conde[a], J. Ferenc[b] and T. Kulik[b] [1]

[a] *Departamento de Física de la Materia Condensada. ICMSE-CSIC. Universidad de Sevilla. P.O. Box 1065. 41080 Sevilla, Spain.*

[b] *Faculty of Materials Science and Engineering, Warsaw University of Technology, ul. Wołoska 141, 02-507 Warsaw, Poland.*

Abstract

Temperature evolution of the coercivity of nanocrystalline samples of $Fe_{60}Co_{18}Nb_6B_{15}Cu_1$ alloy with different crystalline fractions was measured from room temperature up to 690 K. Although room temperature coercivity increases as the nanocrystallization progresses, the thermal stability of the magnetic properties of the system is clearly enhanced as the crystalline volume fraction increases. Microstructure was characterized using room temperature Mössbauer spectra which can be interpreted on the basis of the presence of three different regions: amorphous, crystalline and interface.

PACS codes: 61.46.+w; 75.50.Tt; 75.75.+a

Keywords: Soft magnetic properties, HITPERM, nanocrystalline alloys

Corresponding author: A. Conde

Tel: +34 954 552 885

Fax: +34 954 612 097

e-mail: conde@us.es

Journal of Non Crystalline Solids. Vol. 353. Núm. 8-10. 2007. Pag. 872-874
http://dx.doi.org/10.1016/j.jnoncrysol.2006.12.097

1. Introduction

Partial substitution of Co for Fe in Fe-based nanocrystalline alloys increases the Curie temperature, T_C^{am}, of the amorphous matrix [1], which marks a high temperature limit for the technological applications of these alloys due to the magnetic uncoupling of the α-Fe(Co) nanocrystals above T_C^{am}. On the other hand, the addition of a small amount of Cu refines the microstructure in Nb-containing HITPERM alloys through Cu-clustering phenomenon [2].

As soft magnetic properties of nanocrystalline Fe-based alloys critically depend on microstructure [3], its fine tailoring is of special interest. Besides, a good thermal stability of these properties is necessary when the material is required for applications in a certain temperature range. In this work, thermal and microstructural dependences of the soft magnetic properties of a $Fe_{60}Co_{18}Nb_6B_{15}Cu_1$ alloy are studied for various partially nanocrystallized samples from room temperature (RT) up to 690 K.

2. Experimental

Nanocrystalline samples of $Fe_{60}Co_{18}Nb_6B_{15}Cu_1$ alloy were prepared by heating amorphous melt spun ribbons up to complete a fraction, X_{DSC}, of the first exotherm detected by calorimetry. Samples with X_{DSC} = 0.1, 0.3, 0.6 and 0.9 were studied and in the following they will be named by this value. Thermomagnetic gravimetry (TMG) with an applied field of 20 mT was used to characterize the magnetic transitions. ^{57}Fe RT Mössbauer (MS) spectra were fitted with NORMOS program [4]. The spectra of nanocrystalline samples were fitted using 4 discrete values of hyperfine magnetic field, B_{hyp}, (crystalline contribution) and two B_{hyp} distributions (amorphous phase and interface region).

Journal of Non Crystalline Solids. Vol. 353. Núm. 8-10. 2007. Pag. 872-874
http://dx.doi.org/10.1016/j.jnoncrysol.2006.12.097

High temperature hysteresis loops were recorded using a quasistatic hysteresis loop tracer. The loops were acquired in a continuous heating mode but with a so slow heating rate thus, during the acquisition time (~30 s), the temperature at the sample rose less than 3 K. The absence of microstructural evolution during the measurements was checked. Magnetization, M_S, was obtained at RT for an applied field of 0.5 T in a vibrating sample magnetometer (Lakeshore 7407).

3. Results and discussion

Figure 1 shows the TMG plot of as-cast and partially nanocrystallized samples from which the value of T_C^{am} was obtained (inset). T_C^{am} decreases and becomes less evident as the nanocrystallization progresses. The temperature dependence of coercivity, H_C, appears in Fig. 2. Although RT H_C increases as the nanocrystallization progresses, correlated with the increase of crystalline fraction [5], the thermal stability of the magnetic properties of the system is clearly enhanced as X_{DSC} increases. This stability can be represented by a temperature coefficient of the coercivity, $C^T(H_C)$, analogous to that defined for the permeability [6]:

$$C^T(H_C) = 100\frac{\Delta H_C}{H_C(300K)}\frac{1}{\Delta T} \qquad (1)$$

where ΔH_C is the increment of H_C from the value at 300 K up to the value at T = 300+ΔT K. $C_T(H_C)$, (Fig. 2 inset), varies between ~5 %/K and <0.2 %/K.

A maximum in H_C is clearly observed for the 0.1 sample. For this sample, values of H_C above 660 K could not be measured as the hysteretic signal corresponding to the nanoparticles has a small amplitude preventing the accurate determination of H_C. Above T_C^{am}, the ferromagnetic nanocrystals might behave as weakly interacting superparamagnetic particles embedded in a paramagnetic matrix [7]. For higher crystalline fractions, the maximum in H_C associated with T_C^{am} is not clearly observed,

Journal of Non Crystalline Solids. Vol. 353. Núm. 8-10. 2007. Pag. 872-874
http://dx.doi.org/10.1016/j.jnoncrysol.2006.12.097

due to a stronger interaction between the nanocrystals [7]. A similar effect of X on the thermal stability of H_C has been recently reported for higher Co containing alloys [8]. Figure 3 shows the MS spectra of the nanocrystalline samples. It can be clearly observed how the relative intensity of the crystalline peaks increases as X_{DSC} increases. Along with the experimental data and the total fitting curve, the contribution of the four sextets and that of the two distributions of B_{hyp} are also shown in Fig. 3. The former corresponds to the crystalline Fe sites (ranging from 33.0 T up to 36.8 T). The average values of the hyperfine parameters are the same for the 0.3, 0.6 and 0.9 samples ($<B_{hyp}>$ = 35.6 ± 0.1 T and $<I>$ = 0.037 ± 0.003 mm/s). For the 0.1 sample, $< B_{hyp}>$ = 35.2 T and $<I>$ = 0.049 mm/s but the small amount of crystalline contribution could be responsible for these differences. The use of two distributions of B_{hyp} was proposed in order to distinguish between the contributions of the residual amorphous and the interface region. However, the fitting was ambiguous, due to the similar value of I. Only for the 0.9 alloy, the two contributions could be deconvoluted. In fact, whereas $<B_{hyp}>$ of the amorphous matrix decreases as the crystallization progresses, that of the interface remains constant. Therefore, B_{hyp} contributions above 20 T would correspond to the interface and those below 20 T to the amorphous matrix. For the 0.9 alloy, it is possible to estimate a ratio between the thickness of the interface, δ, and the grain size diameter, D, from the ratio between the areas of the interface and crystalline contributions (A_{Int}~28 % and A_C~49 %, respectively), being δ/D~0.08. For D~5 nm [5], δ~0.4 nm, in agreement with the results obtained for other nanocrystalline compositions [9].

For the 0.1, 0.3 and 0.6 samples, although the interface contribution could not be deconvoluted from that of the amorphous matrix, it was possible to extract some information from the evolution of A_C. Figure 4 shows a linear relationship between both A_C and M_S as a function of X_{DSC}. It is worth noting that extrapolating the value of A_C for

Journal of Non Crystalline Solids. Vol. 353. Núm. 8-10. 2007. Pag. 872-874
http://dx.doi.org/10.1016/j.jnoncrysol.2006.12.097

$X_{DSC} = 0$, A_C is ~12 %. The non-zero value can be explained if the enthalpy per transformed unit associated to the early stages of the nanocrystallization (fractions below 0.1) is smaller than that for fractions above 0.1. This fact can be ascribed to the enhanced nucleation due to the Cu-clustering phenomenon previous to the nanocrystallization which energetically facilitates the initial stages of nanocrystallization. This implies that the nucleation is mainly restricted to X_{DSC} below 0.1 and the subsequent increase of X_{DSC} is mostly due to growth, in agreement with previous kinetic results [10]. Considering a constant value of the interface thickness and imposing a mean grain size $D = 5$ nm for $X_{DSC} = 0.5$, the evolution of A_C yields a change of D from ~4 to ~6 nm for $X_{DSC} = 0.1$ to 0.9.

4. Conclusions

RT H_C of $Fe_{60}Co_{18}Nb_6B_{15}Cu_1$ alloy increases as nanocrystallization progresses but the thermal stability of their magnetic properties is strongly enhanced. Correlation between DSC and MS studies on the evolution of the nanocrystalline microstructure allows a description of the nanocrystallization kinetics: low energy nucleation process of α-Fe phase, due to the Cu-clustering phenomenon previous to the nanocrystallization, is restricted to the early stages of nanocrystallization and a strongly impinged growth process is the main responsible for the rest of the nanocrystallization process.

Acknowledgements-Work supported by the Spanish Government and EU FEDER (Project MAT 2004-04618), the PAI of the Junta de Andalucía and the Centre of Excellence NanoCentre (Warsaw, Poland). J.S.B. acknowledges a research contract from J.A.

Journal of Non Crystalline Solids. Vol. 353. Núm. 8-10. 2007. Pag. 872-874
http://dx.doi.org/10.1016/j.jnoncrysol.2006.12.097

References

[1]. M.E. McHenry, M.A. Willard, D.E. Laughlin, Progress in Mater. Sci. 44 (1999) 291.

[2]. Y. Zhang, J.S. Blázquez, A. Conde, P.J. Warren, A. Cerezo, Mat. Sci. Eng. A 353 (2003) 158.

[3]. A. Hernando, M. Vázquez, T. Kulik, C. Prados, Phys. Rev. B 51 (1995) 3581.

[4]. R. A. Brand, J. Lauer, D. M. Herlach, J. Phys. F: Met. Phys. 12 (1983) 675.

[5]. J.S. Blázquez, V. Franco, A. Conde, J. Phys.: Cond. Matter 14 (2002) 11717.

[6]. J.S. Blázquez, V. Franco, A. Conde, L. F. Kiss, J. Appl. Phys. 93 (2003) 2172.

[7]. V. Franco, C.F. Conde, A. Conde, L.F. Kiss, Phys. Rev. B 72 (2005) 1.

[8]. I. Skorvanek, J. Marcin, T. Krenicky, J. Kovac, P. Svec, D. Janickovic, J. Magn. Magn. Mat. 304 (2006) 203.

[9]. J.S. Blázquez, V. Franco, A. Conde, J. All. Comp. 422 (2006) 32.

[10]. J.S. Blázquez, C.F. Conde, A. Conde, Appl. Phys. A 76 (2003) 571.

Journal of Non Crystalline Solids. Vol. 353. Núm. 8-10. 2007. Pag. 872-874
http://dx.doi.org/10.1016/j.jnoncrysol.2006.12.097

Figure captions

Fig. 1. TMG plots of as-cast and nanocrystalline samples. The inset shows the value of T_C^{am} for each sample. This value could not be measured for the 0.9 sample.

Fig. 2. Coercivity versus temperature for the different nanocrystalline alloys. Inset: thermal coefficient of the coercivity versus nanocrystallization fraction.

Fig. 3. Mössbauer spectra and probability distribution of hyperfine magnetic field contributions of the nanocrystalline samples.

Fig. 4. Saturation magnetization, M_S, and pure crystalline contribution, A_C, as a function of the nanocrystallization fraction.

Journal of Non Crystalline Solids. Vol. 353. Núm. 8-10. 2007. Pag. 872-874
http://dx.doi.org/10.1016/j.jnoncrysol.2006.12.097

Figure 1

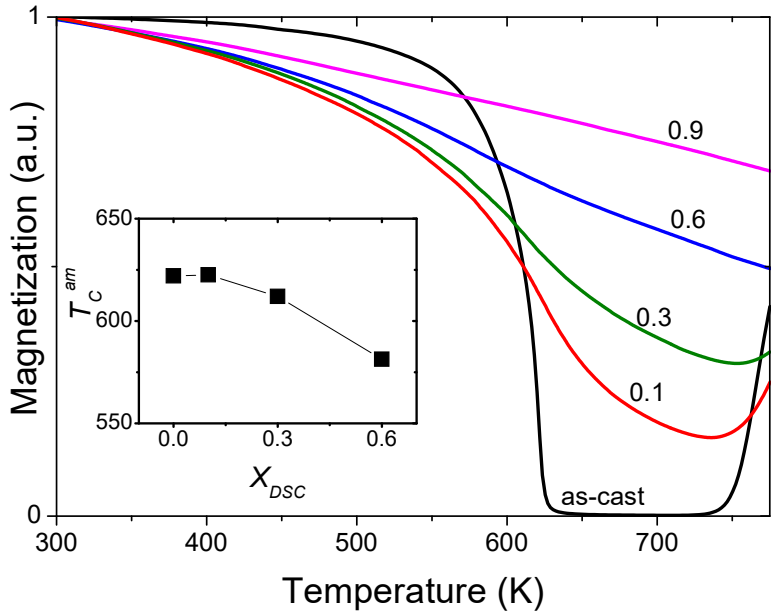

Journal of Non Crystalline Solids. Vol. 353. Núm. 8-10. 2007. Pag. 872-874
http://dx.doi.org/10.1016/j.jnoncrysol.2006.12.097

Figure 2

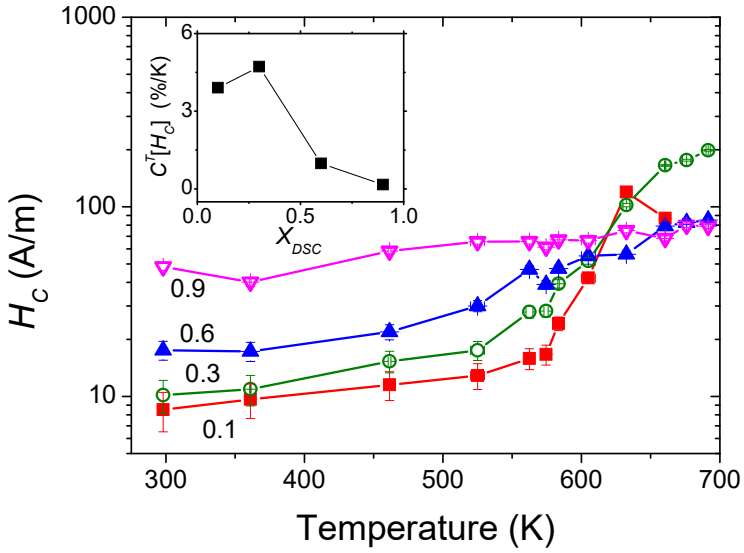

Journal of Non Crystalline Solids. Vol. 353. Núm. 8-10. 2007. Pag. 872-874
http://dx.doi.org/10.1016/j.jnoncrysol.2006.12.097

Figure 3

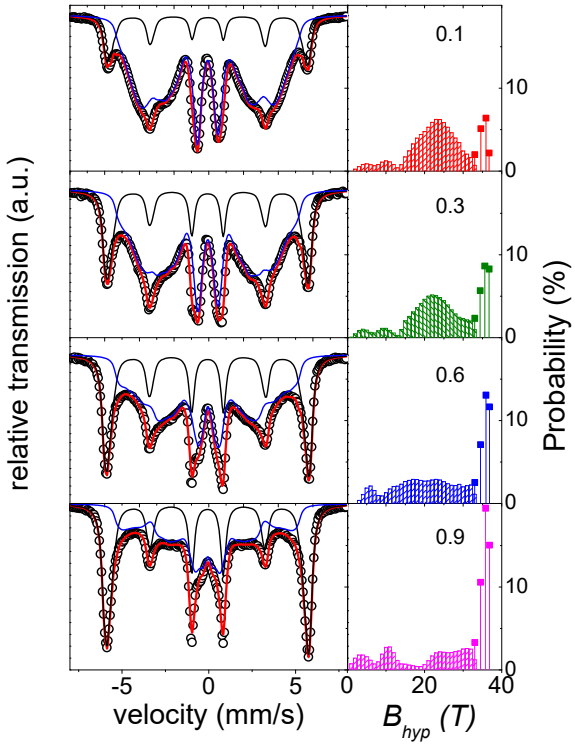

Journal of Non Crystalline Solids. Vol. 353. Núm. 8-10. 2007. Pag. 872-874
http://dx.doi.org/10.1016/j.jnoncrysol.2006.12.097

Figure 4